Pathological fracture risk assessment in patients with femoral metastases using CT-based finite element methods. A retrospective clinical study

Amir Sternheim[1,3], Ornit Giladi[2,3], Yair Gortzak[1,3], MIchael Drexler[2,3], Moshe Salai[2,3], Nir Trabelsi[4], Charles Milgrom[5,*], Zohar Yosibash[6]

[1] National Unit of Orthopaedic Oncology, Tel-Aviv Medical Center, Tel-Aviv, Israel

[2] Division of Orthopaedics, Tel-Aviv Medical Center, Tel-Aviv, Israel

[3] Sackler Faculty of Medicine, Tel-Aviv University, Israel

[4] Dept. of Mechanical Engineering, Shamoon College of Engineering, Beer-Sheva, Israel

[5] Hebrew University School of Medicine, Tzameret, Jerusalem, Israel

[6] School of Mechanical Engineering, Tel-Aviv University, Ramat-Aviv, Israel

*Correspondence to: Professor Charles Milgrom

Hebrew University School of Medicine

Tzameret

Ein Kerem, Jerusalem, Israel, 9112001

E-mail: charlesm@ekmd.huji.ac.il

Key words: metastases; femur; finite element analysis; CTFEA; clinical study

Abstract

Physician recommendation for prophylactic surgical fixation of a femur with metastatic bone disease (MBD) is usually based on Mirels' criteria and clinical experience, both of which suffer from poor specificity. This may result in a significant number of these health compromised patients undergoing unnecessary surgery. CT-based finite element analyses (CTFEA) have been shown to accurately predict strength in femurs with metastatic tumors in an ex-vivo study. In order to assess the utility of CTFEA as a clinical tool to determine the need for fixation of patients with MBD of the femur, an ad hoc CTFEA was performed on a retrospective cohort of fifty patients.

Patients with CT scans appropriate for CTFEA analysis were analyzed. Group 1 was composed of 5 MBD patients who presented with a pathologic femoral fracture and had a scan of their femurs just prior to fracture. Group 2.was composed of 45 MBD patients who were scheduled for a prophylactic surgery because of an impending femoral fracture. CTFEA models were constructed for both femurs for all patients, loaded with a hip contact force representing stance position loading accounting for the patient's weight and femur anatomy. CTFEA analysis of Group 1 patients revealed that they all had higher tumor associated strains compared to typical non-diseased femur bone strains at the same region (> 45%).

Based on analysis of the 5 patients in Group 1, the ratio between the absolute maximum principal strain in the vicinity of the tumor and the typical median strain in the region of the tumor of healthy bones (typical strain fold ratio) was found to be the 1.48. This is considered to be the predictive threshold for a pathological femoral fracture. Based on this

typical strain fold ratio, twenty patients (44.4%) in Group 2 were at low risk of fracture and twenty-five patients (55.5%) high risk of fracture.

Based on CTFEA, 39% of the patients with femoral MBD who were referred and underwent prophylactic stabilization may not have needed surgery. On the basis of these results a prospective randomized clinical trial evaluating CTFEA as a criterion for determining the need for surgical stabilization in patients with MBD of the femur may be warranted.

Introduction

Between one third to one half of all cancers metastasize to bones (1). In 30- 50% of the cases metastatic bone disease (MBD) weakens the bone's structure and may lead to pathologic fractures under daily physiological loading or pain symptoms severe enough to require treatment (2). As a result of new immuno-oncological and chemotherapy treatments, patients with MBD are living longer (3). More than 280,000 new cases of long bone skeletal metastases are reported in the United States every year (4). Weight bearing bones, specifically the femur, are at highest risk of pathologic fracture. For suspected impending femoral fractures, prophylactic fixation is the recommended treatment because it has less morbidity and mortality than actual fracture surgery which occurs after the trauma triggers a cascade of adverse hemodynamic, metabolic and neuro-endrocrince events (3, 5). The cost of prophylatic femoral fixation is $78,000/patient (7). Economic impact studies have shown that the cost of prophylactic femoral fixation for a MBD patient is $21,000 less than if treatment is given post fracture (6). Unnecessary prophylactic surgery can cause morbidity and require lengthy patient rehabilitation period. Effective management of patients with MBD depends on patient-specific accurate assessment of the risk of fracture.

Using clinical judgment to predict pathologic fracture risk is in many ways a learned art. Orthopedic surgeons are often expected to assess this risk in the setting of disseminated metastatic disease with bone involvement. They have to identifying those who are at high risk of fracture and those who are not. Although clinical judgment has been shown to be a suboptimal tool, its strength is in its ability to account for change in pain over time. A patient

with increasing pain over time is considered to have an increasing probability of fracture. Plain radiographs are not sensitive or specific enough to make this prediction (8, 9). Based on radiographs, experts tend to overestimate fracture risk (10). Fracture prediction based on radiographs is further complicated in patients with permeative or diffuse lesions without clear margins. Dijkstra et al. (1997) were not able to perform an accurate measurement in such cases in 50% of patients (27 out of 54 patients) (11).

Mirels' system (12) classifies the risk of pathologic fractures related to MBD based on pain, location of lesion, size of cortical destruction, and the appearance of the lesion (lytic vs. blastic). Each feature is assigned progressive scores ranging from 1 to 3 and the scores are summated. Patients with a score above 8 are considered to be at high fracture risk and in need of prophylactic fixation. Mirels' classification has been shown to be reproducible, valid and more sensitive than clinical judgment, but its low specificity (35%) may result in unnecessary surgery in two thirds of the patients (2, 13, 14). In a cohort of 102 patents with painful femoral metastases, Mirels' score correctly predicted fracture in all 14 patients who fractured, but also predicted fracture in 84 out of 88 patients who did not fracture (10). Mirels' classification is therefore more valid as a screening tool given its sensitivity (2).

In recent years more accurate methods based on either rigidity analysis or finite element models generated from computed tomography (CT) scans have been suggested as a means to predict bone strength that account for both patient specific geometrical structure and spatial distribution of material properties in bones with metastases (15-18). A patient-

specific CT-based finite element analysis (CTFEA) has been double-blinded validated in ex-vivo experiments using fresh-frozen femurs (19). Employing the same CTFEA method, CTFEA predictions were compared to experimental mechanical tests in 14 fresh frozen femurs with real metastatic tumors (15). The study showed that CTFEA predicts the mechanical response of femurs with metastases with a linear regression slope of 0.95 and a coefficient of linear regression R^2= 0.967. A good correlation was demonstrated between the predicted yield load and experimental observed yield, with a linear regression slope of 0.80 and a coefficient of linear regression R^2= 0.78 (17).

A recent systematic review (14) addressed the different methods for fracture risk evaluation in patients with femoral metastases. It concludes that *“Fracture risk prediction using Mirels' score, based on pure clinical data, shows moderate to poor results in predicting non-impending fractures with a positive predictive value between 23 and 70%. Engineering methods provide high accuracy in biomechanical lab experiments, but have not been applied to clinical routine yet... ".*

Given that Mirels’ classification combined with clinical judgment has a low specificity rate, and the successful correlation between CTFEA and ex-vivo experiments, we hypothesize that personalized CTFEA may be significantly more specific at predicting the need for prophylactic surgery in patients with femoral MBD. To clinically validate the

hypothesis we performed an ad hoc CTFEA retrospectively on a cohort of 50 patients with femoral MBD compared to Mirels' scores and clinical outcome data.

Materials and Methods

Patients

Records of 157 patients with metastatic tumors of their femurs referred to the National Unit of Orthopedic Oncology Center at Tel-Aviv Medical Center during March 2013 – March 2017 were reviewed. Institutional review board approval (# 0530-15-TLV) to retrospectively perform a review of patient clinical records was received. Weight, gender, type of primary cancer and CT date were collected for each patient. To be included in the study patients were required to have a CT extending from the femoral head to at least 1cm below the femoral less trochanter, with a tube current of 120kVp, with a pitch <1.5mm and an appropriate filter. Decisions regarding surgery were approved by hospital's tumor board consisting of 4 surgeons and a musculoskeletal radiologist, based on clinical and radiographic judgment.

Fifty-seven patients were referred after already experiencing a pathological fracture. Five of these patients had an appropriate CT scan within a month prior to the fracture. All 5 sustained spontaneous fractures. These 5 patients form Group 1. In four of the five patients their CT scan included the entire femur and their contralateral, non fractured femur was judged to be disease free.

One hundred patients were recommended prophylactic fixation because of high risk of impending pathologic fractures based on Mirels' scoring done by two orthopaedic surgeon and their clinical judgement. Forty-five of these had an appropriate CT scan. These patients form study Group 2. Twelve of the 45 patients chose not to have the recommended surgery. One of the twelve was confined to bed rest from the time of the surgical recommendation until his death three months later. Eight of the 45 patients had CT scans which included the entire femurs and their contralateral non symptomatic femur was judged to be disease free.

There was no statistically significant difference (p=0.9) between subjects years of age in Group 1 (63.6±7.3) and Group 2 (62.7±15) or between subject weight (p=0.65) in Group 1 (72.4±9.7 kg) and Group 2 (78±26.7 kg) . 3/5 of the patients in Group 1 and 28/45 in Group 2 were females (p=0.36) . Details of the tumor origin for the two groups are presented in Table 1.

Table 1 – Number of patients and tumor origin of metastasis in each group

Group One			Number of Patients
	Tumor Origin of Metastasis	Multiple Myeloma	3
		Lung	1
		Adenocarcinoma intrauterine	1
		Total	5 (2M, 3F)
Group Two			Number of Patients
	Tumor Origin of Metastasis	Breast	14
		Multiple Myeloma	9
		Lung	6
		Renal Cell Cancer	6
		Prostate	2
		Other	8
		Total	45 (17M, 28F)

Two orthopaedic oncology surgeons independently scored the patients based on Mirels' criteria for this study. The correlation coefficient was calculated for their assessments. The summary of all cases including gender, age, weight, cancer type, Mirels' score and whether the patient had a prophylactic surgery is presented in *Appendix A*. All tumors in Groups 1 and 2 were either lytic or permeative. All patients were treated in the same orthopedic oncology unit and had a minimum follow-up of four to five months post CT scan unless marked by an *.

CTFEA

High order FE models of the patients' femurs were constructed based on the CT according to the algorithm previously published (17) and schematically illustrated in Figure 1. Briefly, the geometry of the femurs was segmented from the CT-scans and inhomogeneous isotropic material properties were assigned to all points within the femur based on the Hounsfield Unit (HU) in the CT scan.

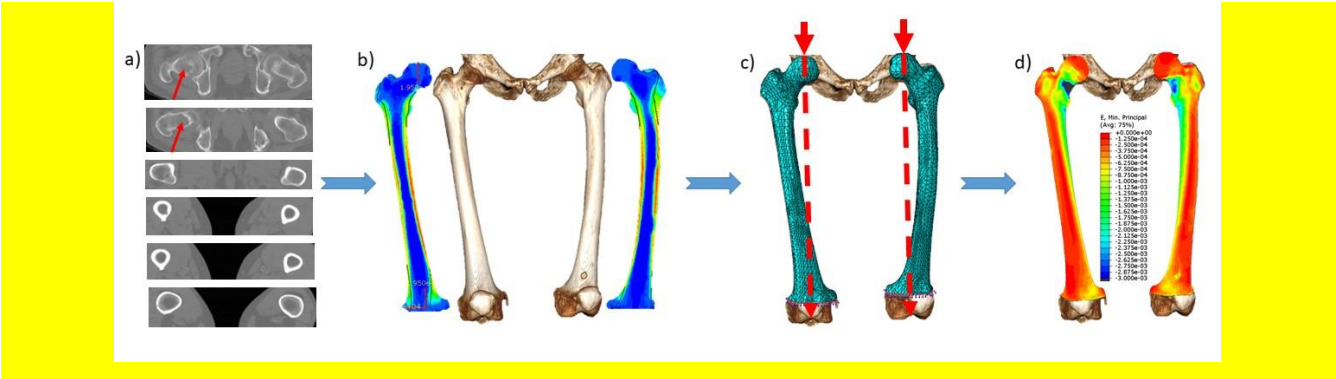

Figure 1 – Schematic algorithm for generating the patient-specific FE model of the femur. a) CT scan of the two femurs (arrow point at the tumor location), b) The 3-D segmented femurs and a cross section showing the E-modulus within the femurs, c) FE mesh and application of stance position loading conditions, d) Compressive maximum principal strains.

For all patients (except very few that already had an implant in the contralateral femur) CTFEA has been performed for both femurs..A load that represents stance position was applied on the femoral head having a magnitude of approximately 2.5 body weight (20) directed along the line connecting the center of the femur head to the intercondylar region of the distal femur. Clamped boundary conditions were applied to the distal part of the femur.

In cases in which the CT scan includes only the proximal femur, the most distal CT slice is clamped and load is applied at an angle approximately 7 degrees to the shaft axis. In all cases the resulting force and moment at the clamped slice and at mid shaft of both femurs were compared to ensure similar results.

Material properties assigned to the FE model:

Using relationships between Young's modulus and ash density for cortical (21) and trabecular bone (22), validated in (17), the following relations were used to determine Young's modulus in the femur:

$$\rho_{K2HPO4} = 10^{-3}\,(a \times HU + b) \qquad [grm/cm^3] \qquad (1)$$

$$\rho_{ash} = 0.877 \times 1.21 \times \rho_{K2HPO4} + 0.08 \qquad [grm/cm^3] \qquad (2)$$

$$E_{cort} = 10200 \times \rho_{ash}^{2.01}\ [MPa], \qquad \rho_{ash} \geq 0.486\ [grm/cm^3] \qquad (3)$$

$$E_{trab} = 2398\ [MPa], \qquad 0.3 < \rho_{ash} < 0.486\ [grm/cm^3] \qquad (4)$$

$$E_{trab} = 33900 \times \rho_{ash}^{2.2}\ [MPa], \qquad \rho_{ash} \leq 0.3\ [grm/cm^3] \qquad (5)$$

The Poisson ratio was set to the constant value of $\nu = 0.3$ (23),(17). The pointwise Young modulus based on CT grey level (surrogate to bone density) is commonly obtained by calibration phantoms (containing several concentration of Dipotassium Phosphate (K_2HPO_4)) scanned along with patient's femur (see eq. (1)). However, because most of the clinical CT scans were performed without calibration phantoms, we estimated the linear relation between HU and bone density without phantoms based on conclusions drawn in previous experimental studies:

1. Maximum bone density (along the entire femur) for all patient regardless of age and gender is almost constant.

2. As a result, the maximum Young's modulus regardless of age and gender is almost constant.

3. HU=0 is related to ash density=0 (i.e. *b=0* in eq. (1)).

The maximum Young's modulus is based on six relevant studies presented in Table 1 in reference (24). Since the longitudinal Young modulus is of interest, and based on data obtained in our previous experimental work we set the maximum Young's modulus to 20GPa. Using E_{max} = 20 GPa in (3), $(\rho_{ash})_{max}$ is computed. Inserting $(\rho_{ash})_{max}$ in (2) $(\rho_{K2HPO4})_{max}$ is computed. Since *b*=0 in (1) by assumption 3 above, we may determine *a* by using $(\rho_{K2HPO4})_{max}$ and if HU_{max} would be known. HU_{max} in patient's CT scan must be extracted from the CT scan of the femur. It is given in the segmented femur's file after one considers the histogram of the HU in CT's voxels. HU_{max} is the value above which there are only 0.1% of the voxels in an entire femur. Using HU_{max} together with $(\rho_{K2HPO4})_{max}$ in (1) the linear slope parameter *a* is determined and finally one may use relationships (2) to (5) to evaluate the material properties for all pixels and for all HUs.

The femur's response under physiological stance position loading is well described by the linear theory of elasticity and although the bone on the macroscopic level is orthotropic, excellent results have been obtained using isotropic inhomogeneous relations for stance position loadings (see (17, 23) and references therein). Therefore, a linear finite element analysis was performed to both femurs. Verification of the numerical results was performed

by monitoring the error in energy norm and the maximum and minimum principal strains at the locations of interest.

Estimation of femur strength and fracture risk

To evaluate the relative bone strength at tumor surroundings compared to non-diseased femurs we used the CTFEA predicted principal strains. Using the 12 subjects whose contralateral hip was judged to be disease free and whose CT scans included the entire femur, we first calculated the median tensile or compressive principal strain at 4 regions of the femur (neck, proximal shaft, middle shaft, distal shaft) of the disease free femurs (4 patients from Group 1 and 8 from Group 2). The ratio between the absolute maximum principal strain in the vicinity of the tumor and the typical median strain in the same anatomical region of the disease free femurs was calculated and denoted *typical strain fold ratio*. As another measure of the femur strength at the tumor region we calculated the ratio between the tensile and compressive strains at the tumor surroundings and the strain in the same region in the contralateral disease free femur denoted by *contralateral strain fold ratio*.

Statistical Analysis

Comparison of patient demographics of Groups 1 and 2 was done by the Student's *t*-test. The correlation between patient MIrels' scores and the typical strain fold ratio values was assessed by the Pearson correlation. The agreement between the Mirels' scoring for the two observers was performed by calculation the interclass correlation coefficient.

Results

CTFEAs were performed for all 50 patients in Table 1. Examples of the CTFEA are shown in Figures 2-4. The interclass correlation coefficient for the Mirels' scoring for the two observers = 0.928.

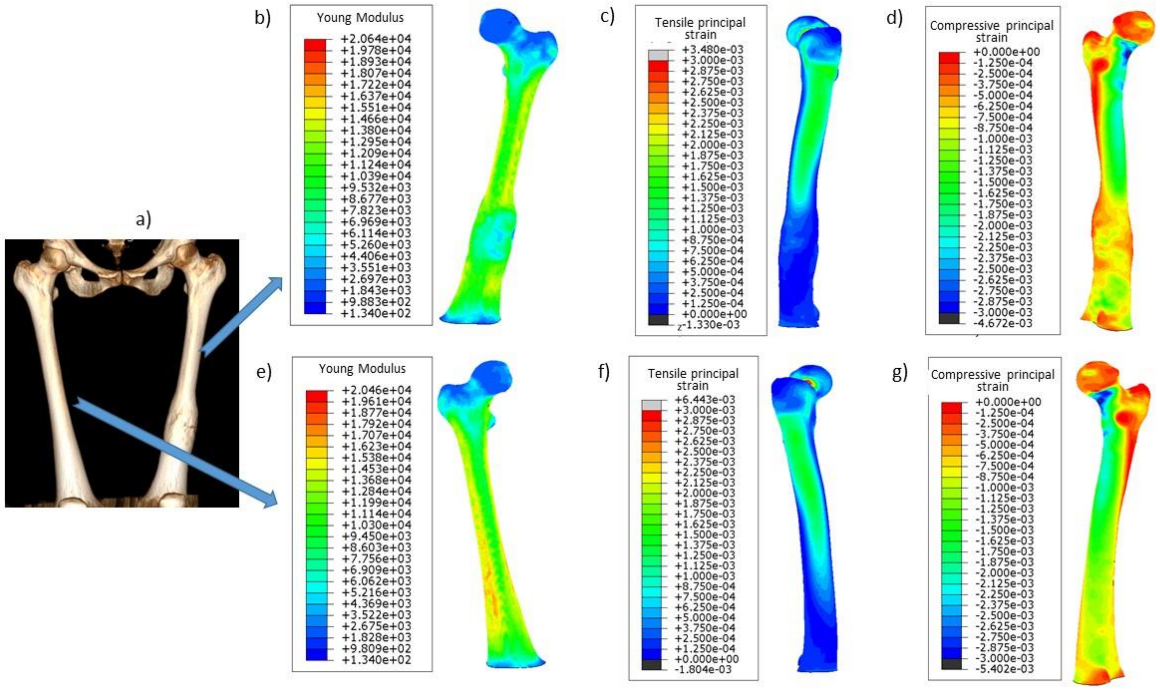

Figure 2 – CTFEA of femurs of a 39 y.o., 70kg, female with lung metastatic tumors in the left femur, Mirels score 7 (patient 32) – illustrative example of comparison between left b-d) and right intact femurs e-g) at 2.5 body weights stance position. a)&e) Young modulus distribution c)&f) tensile principal strains, and d)&g) compressive principal strains.

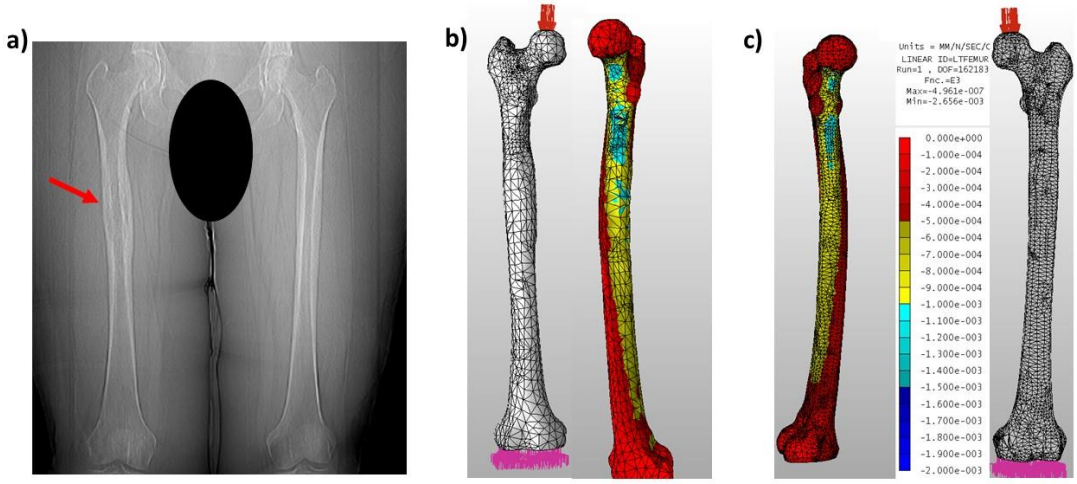

Figure 3 – Radiograph and CTFEA of a 43 y.o., 120kg female with breast cancer metastatic tumors in the right femur with a Mirels' score of 10 (patient 1), but CTFEA results show low fracture risk. This example shows a permeative lesion, with significant changes in the cortexes in a large diaphyseal lesion- all these parameters are not well defined with Mirels classification. a) Radiograph. b)&c) CTFE model and maximum compressive principal strains at 2.5 body weights stance position. Colors represent the maximum compressive principal strains – hot colors are high strains.

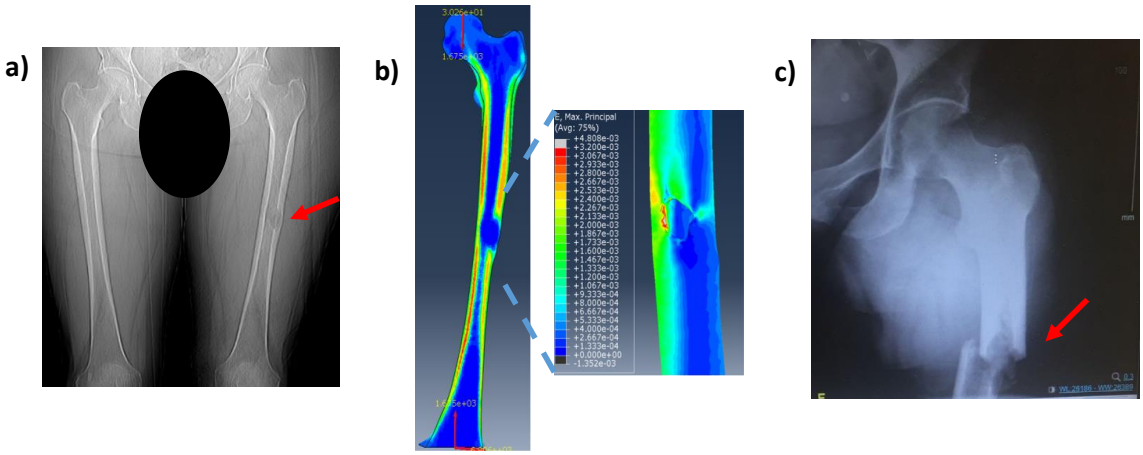

Figure 4 – Radiographs and CTFEA of a 54 y.o., 67kg female with uterine sarcoma (lytic) tumor in mid diaphysis in the left femur with a Mirels' score of 8 and an estimation of a low risk of fracture (patient pathological fracture 4) but the CTFEA predicted a high risk of fracture. The patient experienced a pathological fracture within 3 weeks after the CT scan. a) Radiograph prior to fracture, b) CTFEA model and maximum principal tensile strains at 2.5 body weights stance position. Colors represent the maximum tensile principal strains – hot colors are high strains. c) Radiograph after the pathological fracture

The median maximum principal strains of the contralateral disease free femurs in 12 patients who had CT scans of their entire femurs are presented in Table 2. Half the patients were female and half male. Their age range was 26-80 years of age and their weight range was 45-175 kg. Details of these patients can be found in the Appendix (reference numbers: 16, 22, 23, 31, 39, 40, 43, 44, B1, B2, B3, B4),

Table 2 - Typical tensile and compressive principal strains (μstrain) at the four distinct regions of the femur

Femur region	Tensile strain (μstrain)	Compressive strain (μstrain)
Neck	2850	2750
Proximal shaft	1375	2100
Middle shaft	1325	1850
Distal shaft	625	1100

All 5 patients from Group 1 showed absolute increases of more than 48% in tumor associated strains compared to typical strains at the same region in disease free femurs . The typical strain fold ratios were in the range of 1.48 to 2.41. When the strains were compared to the contralateral strains, the increase was smaller (contralateral strain fold ratio 1.25-2.00), possibly because the contralateral bone itself has somewhat diminished bone strength. The 1.48 typical strain fold ratio value was used as the determinant of the threshold for pathological femoral fracture. The typical strain fold ratio and Mirels' score of each of the 50

patients in the study is given in Appendix A . Figure 2 shows a CTFEA of both femurs of a patient for whom low fracture risk is predicted.

Seventeen out of the 50 patients did not undergo prophylactic surgery after having CT scans and continued to perform activities of daily living. They effectively represent those who underwent mechanical testing of their MBD affected femurs. One of the 12 patients who was recommended prophylactic surgery but declined, was excluded from further analysis because he was hospitalized after the CT scan and was at bed rest until his death 3 months later. Since the 5 subjects of Group 1 were used to calculate the typical strain fold ratio threshold they are not included in the assessment of the accuracy of the CTFEA model. None of the 11 remaining patients who declined surgery after it was recommended, sustained pathological fractures of their femurs. According to CTFEA using the 1.48 typical strain fold ratio threshold, 7 patients were below the pathological fracture threshold and four above, for a specificity of 63%. Since there were no fractures sensitivity cannot be calculated. The correlation coefficient for Mirels' score and the strain fold values for the 11 patients was 0.81.

Using the 1.48 typical strain fold ratio threshold value, CTFEA determined that (44%) patients 20/45 who were indicated for prophylactic surgery were at low fracture risk. Thirteen out of the 33 patients who actually underwent prophylactic surgery were predicted according to the CTFEA model to have low fracture risk. This indicates that 39% of the surgeries may not have been necessary.

Of the five patients in Group 1, only one had a MIrels' score above 8 for which the Mirels' classification recommends prophylactic surgery . The radiographs and CTFEAs for Goup 1 are shown in *Appendix B*.

Discussion

In this study a 1.48 typical strain fold ratio was used as the determinant of the threshold for pathological femoral fracture in cases of femoral MBD. The value was determined based on CTFEA of 5 cases in the study cohort who sustained pathological fracture and had CT scans no more than one month prior to fracture which were of sufficient quality to perform the analysis. The strain fold ratio is the ratio between the absolute maximum principal strain in the vicinity of the tumor under study and the typical median strain in the same anatomical region of the disease free femurs. It was found that comparing the results of the MDB affected femur to their own contralateral femur resulted in lower ratios, probably because the contralateral bone was also affected to some extent by MBD and therefore weaker.

The 11 patients in the study cohort who were recommended prophylactic surgery based on MIrels criteria, but declined operation and continued to perform activities of daily living, effectively underwent mechanical testing of their MDB affected femur. None of these

patients fractured. The specificity of the CTFEA using the 1.48 threshold typical strain fold ratio for these patients was 63 per cent. When the same threshold criteria was applied to study patients who underwent prophylactic surgery it was found that 39% may have undergone unnecessary surgery. In this sick population, such unnecessary surgery can cause unnecessary pain, suffering, complications and economic expenses.

It is generally accepted that current treatment decisions regarding prophylactic fixation for patients with femoral MBD are of low specificity. Piccioli et al.:stated that: " A consistent tool to evaluate impending fractures would be of great value to guide the treatment of metastatic bone disease" (25). CTFEA has been shown to accurately predict the bone strength in ex-vivo experiments on fresh frozen human femurs with metastatic lesions (17).The present retrospective study demonstrates the ability of the technique to make femoral strength predictions clinically.

Maximum CTFEA specificity may not have been achieved in this study because CT data were from different CT scanners, performed without a calibration phantom, and some were done with protocols that were suboptimal for analysis. In this study fracture risk was determined on the basis of a 4-5 month clinical follow-up with CTFEA having a 63% sensitivity. Two of the patients for whom fracture was predicted did not fracture during the initial observation period, but experience a pathological fracture thru their lesion subsequently. Two of the four patients who for which CTFEA predicted a high risk of fracture and did not experience a fracture within the 5 month observation period, did eventually experience a pathological fracture in spite of preventive medical treatment (one after a year and another after almost 2 years after their CT scans). If these cases would had been

included in our analysis, the specificity of CTFEA would had risen to 82%. Our observations are supported by a recent prospective clinical study. Using low order FEA (26) the authors analyzed 11 cases that were prophylactic stabilized and conclude that “a large fraction of these cases would not be predicted to fracture, despite the high Mirels score (10).”

Similar to CTFEA, an alternative method to predict the risk of fracture is the CT based rigidity analysis (CTRA) (15, 27). CTRA is a simplified method focusing on comparison of 2-D CT slices with respect to “local rigidity”. Although it does not account for patient-specific physiological loading, the 3D geometry of the femur and specific fracture criteria of bone, it has been shown to be superior to Mirels score in specificity (15). CTRA it is not appropriate in cases in which the patient has a femoral orthopedic implant because of the test's intrinsic requirement of comparison between right and left femurs. It also may be inaccurate if the tumor is in a region where the beam theory has poor representation of the bone domain such as the intertrochanteric region . An advantage of CTRA’s is the short analysis time, however with the development of semi-automatic methods the CTFEA is nowadays performed within a framework of 4 hours. CTFEA and CTRA have been compared in an ex vivo study using simulated lytic bone defects *(*28), but not for bones with real tumors as has been done for CTFEA.(17). Future studies need to be performed to compare CTRA and CTFEA predictions for clinical applications.

Several limitations are associated with the ad hoc retrospective nature of this study: 1) Selection bias may be present because only a third of the patients who presented to the study clinic with femoral MBD had the necessary CT to perform CTFEA analysis;. 2) The typical strain fold ratio threshold for pathological fracture was calculated based on only 5

patients who fractured and 12 normal femurs; 3) The study control group was composed ad hoc from patients who declined surgery; 4) The CT scans were not optimized to CTFEA. They were performed without calibration phantoms, with different filters, and in some cases only a small part of the femur was imaged. A prospective study with proper standardized CT scans could possible optimize the full potential of this technology.

Conclusion

Although retrospective, this is the first clinical study to the best of our knowledge that uses validated finite element technology, and indicates that CTFEA may be superior to the current standard methods used to evaluate the need for prophylactic surgery in patients with femoral metastases. The outcome of this study encourages us to proceed to the next step, a randomized prospective clinical trial with a control group. The outcome of such a clinical study will be utilized to substantiate the use of CTFEA for patients with femoral MBD.

Conflict of Interest Statement

NT, CM, and ZY have a financial interest in PerSimiO, and both they and the company may benefit from the results of this research. All the other authors state that they have no conflicts of interest.

References

1. Coleman RE. Clinical features of metastatic bone disease and risk of skeletal morbidity. Clin Cancer Res. 2006;12(20 Pt 2):6243s-9s.

2. Jawad MU, Scully SP. In brief: classifications in brief: Mirels' classification: metastatic disease in long bones and impending pathologic fracture. Clin Orthop Relat Res. 2010;468(10):2825-7.

3. Mavrogenis AF, Pala E, Romagnoli C, Romantini M, Calabro T, Ruggieri P. Survival analysis of patients with femoral metastases. J Surg Oncol. 2012;105(2):135-41.

4. Cheung FH. The practicing orthopedic surgeon's guide to managing long bone metastases. Orthop Clin North Am. 2014;45(1):109-19.

5. Ratasvuori M, Wedin R, Keller J, Nottrott M, Zaikova O, Bergh P, et al. Insight opinion to surgically treated metastatic bone disease: Scandinavian Sarcoma Group Skeletal Metastasis Registry report of 1195 operated skeletal metastasis. Surg Oncol. 2013;22(2):132-8.

6. Gendi K, Hennessy D, Heiner J. The burden of metastatic disease of the femur on the Medicare system. Springerplus. 2016;5(1):1916.

7. Blank AT, Lerman DM, Patel NM, Rapp TB. Is Prophylactic Intervention More Cost-effective Than the Treatment of Pathologic Fractures in Metastatic Bone Disease? (vol 474, pg 1563, 2016). Clin Orthop Relat R. 2016;474(7):1742-3.

8. *Damron TA, Ward WG. Risk of pathologic fracture: assessment. Clin Orthop Relat Res. 20*03(415 Suppl):S208-11.

9. Haidukewych GJ. Metastatic disease around the hip: maintaining quality of life. J Bone Joint Surg Br. 2012;94(11 Suppl A):22-5.

10. Van der Linden YM, Dijkstra PD, Kroon HM, Lok JJ, Noordijk EM, Leer JW, et al. Comparative analysis of risk factors for pathological fracture with femoral metastases. J Bone Joint Surg Br. 2004;86(4):566-73.

11. Dijkstra PD, Oudkerk M, Wiggers T. Prediction of pathological subtrochanteric fractures due to metastatic lesions. Arch Orthop Trauma Surg. 1997;116(4):221-4.

12. Mirels H. Metastatic disease in long bones. A proposed scoring system for diagnosing impending pathologic fractures. Clin Orthop Relat Res. 1989(249):256-64.

13. Damron TA, Morgan H, Prakash D, Grant W, Aronowitz J, Heiner J. Critical evaluation of Mirels' rating system for impending pathologic fractures. Clin Orthop Relat Res. 2003(415 Suppl):S201-7.

14. Benca E. The insufficiencies of risk analysis of impending pathological fractures in patients with femoral metastases: A literature review. Bone Reports. 2016;5:51-6.

15. Damron TA, Nazarian A, Entezari V, Brown C, Grant W, Calderon N, et al. CT-based Structural Rigidity Analysis Is More Accurate Than Mirels Scoring for Fracture Prediction in Metastatic Femoral Lesions. Clin Orthop Relat Res. 2016;474(3):643-51.

16. Derikx LC, van Aken JB, Janssen D, Snyers A, van der Linden YM, Verdonschot N, et al. The assessment of the risk of fracture in femora with metastatic lesions: comparing case-specific finite element analyses with predictions by clinical experts. J Bone Joint Surg Br. 2012;94(8):1135-42.

17. Yosibash Z, Plitman Mayo R, Dahan G, Trabelsi N, Amir G, Milgrom C. Predicting the stiffness and strength of human femurs with real metastatic tumors. Bone. 2014;69:180-90.

18. Derikx LC, Verdonschot N, Tanck E. Towards clinical application of biomechanical tools for the prediction of fracture risk in metastatic bone disease. J Biomech. 2015;48(5):761-6.

19. Trabelsi N, Yosibash Z, Wutte C, Augat P, Eberle S. Patient-specific finite element analysis of the human femur-A double-blinded biomechanical validation. Journal of Biomechanics. 2011;44(9):1666-72.

20. Yosibash Z, Wille H, Rank E. Stochastic description of the peak hip contact force during walking free and going upstairs. J Biomech. 2015;48(6):1015-22.

21. Keller TS. Predicting the compressive mechanical behavior of bone. Journal of biomechanics. 1994;27(9):1159-68.

22. Keyak JH, Fourkas MG, Meagher JM, Skinner HB. Validation of an automated method of three-dimensional finite element modelling of bone. Journal of biomedical engineering. 1993;15(6):505-9.

23. Yosibash Z, Trabelsi N, Milgrom C. Reliable simulations of the human proximal femur by high-order finite element analysis validated by experimental observations. J Biomech. 2007;40(16):3688-99.

24. Trabelsi N, Yosibash Z. Patient-Specific Finite-Element Analyses of the Proximal Femur with Orthotropic Material Properties Validated by Experiments. J Biomech Eng-T Asme. 2011;133(6).

25. Piccioli A, Spinelli MS, Maccauro G. Impending fracture: A difficult diagnosis. Injury. 2014;45 Suppl 6:S138-41.

26. Goodheart JR, Cleary RJ, Damron TA, Mann KA. Simulating activities of daily living with finite element analysis improves fracture prediction for patients with metastatic femoral lesions. J Orthop Res. 2015;33(8):1226-34.

27. Nazarian A, Entezari V, Villa-Camacho JC, Zurakowski D, Katz JN, Hochman M, et al. Does CT-based Rigidity Analysis Influence Clinical Decision-making in Simulations of Metastatic Bone Disease? Clin Orthop Relat Res. 2016;474(3):652-9.

28. Anez-Bustillos L, Derikx LC, Verdonschot N, Calderon N, Zurakowski D, Snyder BD, et al. Finite element analysis and CT-based structural rigidity analysis to assess failure load in bones with simulated lytic defects. Bone. 2014;58:160-7.

Appendix A – Summary of cases including gender, age, weight, cancer type, Mirel's score, CTFEA risk of fracture and outcome.

Group 1

#	Mirels 1	Mirels 2	Max strain fold ratio	Tumor region	M/F	Cancer type**	Age	BW (kg)	Height	R/L	Part of Femur in CT	R/L Difference	Scanner	kVp	FilterType
B1	9	?	1.48	Neck	F	MM	59	68	160	R	166 mm Proximal	14%	Philips-59640ed	140	Bone
B2	7	8	2.27	Distal shaft	M	MM	75	75	165	L	Entire	67%	Philips Briliance 64	120	D - Bone
B3	7	8	2.27	Distal shaft	F	MM	68	62	152	L	Entire	75%	Philips Briliance 64	120	B
B4	8	8	1.89	Middle shaft	F	AI	54	67	163	L	Entire	20%	Philips Core Ingenuity	120	A
B5	8	?	1.71	Neck	M	L	62	90	?	R	150 mm proximal	47%	Philips Core Ingenuity	120	A

** MM – Multiple myeloma, L – Lung, AI – Adenocarcinoma intrauterine

Group 2

#	Mirels 1	Mirels 2	Max strain fold ratio	Tumor region	M/F	Cancer type**	Age	BW (kg)	Height	R/L	Part of Femur in CT	R/L Difference	Scanner	kVp	FilterType	Operated*
1	10	10	0.75	Middle shaft	F	B	43	120	173	L	Entire		Philips Briliance 64	140	Bone-D	y
2	7	7	1.35	Middle shaft	M	P	89	80	?	L	187 mm SHAFT only	Implant	Philips iCT256	120	Soft-B	n
3	11	11	2.33	Middle shaft	F	Tyroid	75	70	155	R	Entire	250%	Siemens Somatom	120	B60f	y
4	11	11	3.63	Proximal shaft	F	MM	70	79	178	R	Entire	27%	Philips iCT256	120	YB-Soft	y
5	11	12	3.63	Proximal shaft	M	Thimic Carcin.	17	79	175	L	142 mm Proximal	450%	Philips iCT256	120	YD-Bone	y
6	10	10	0.90	Neck	F	B	41	55	160	L	Entire	15%	Philips Briliance 64	120	YD-Bone	y
7	11	12	2.18	Proximal shaft	F	B	46	45	163	R	126mm Proximal	150%	Siemens	140	B60s-sharp	y
8	11	10	1.67	Proximal shaft	M	RCC	56	88	176	R	Entire	30%	Philips Briliance 64	120	Soft-B	y
9	10	10	4.48	Distal shaft	F	L	70	55	160	L	Entire	25%	Philips Briliance 64	120	Soft-B	y
10	11	11	0.95	Proximal shaft	F	B	66	105	161	R	122 mm Proximal	50%	Philips iCT256	120	Soft-B	y

11	10	10	2.70	Middle shaft	F	Transitional Cell Carcin.	79	54	152	R	Entire	456%	Philips Briliance 64	120	Soft-B	y
12	9	10	3.63	Proximal shaft	F	B	60	75	160	L	Entire	210%	Siemens Somatom	100	Bone - B70f	y
13	9	10	1.09	Neck	M	P	95	90	180	R	about 101 mm Proximal	33%	Philips Briliance 64	120	Soft-B	y
14	10	11	1.67	Proximal shaft	M	MM	57	107	175	R	Entire	18%	Philips Briliance 64	120	Bone - B70f	y
15	9	10	3.63	Proximal Shaft	M	RCC	71	65	175	R	177 mm Proximal	370%	GE Discovery CT750 HD	120	Bone Plus	y
16	11	11	4.00	Distal shaft	M	MM	80	75	153	R	Entire	4400%	Philips iCT256	120	B-soft	n
17	11	11	1.50	Neck	M	RCC	75	70	172	L	115 mm Proximal	100%	GE Discovery CT750 HD	120	standard	y
18	10	10	2.00	Neck	F	L	64	78	165	R	Entire	169%	Philips Mx8000 IDT 16	120	A	y
19	6	6	1.34	Neck	F	Not Clear	70	72	150	R	84 mm Proximal	3%	Philips Briliance 64	120	B-soft	y
20	11	11	1.23	Neck	M	L	60	90	180	L	Entire	380%	Siemens Somatom	120	B30f	y
21	10	10	1.14	Proximal shaft	F	B	74	73	155	L	Entire	Implant	Philips Briliance 64	120	A	n
22	11	11	3.68	Distal shaft	M	RCC	71	170	198	L	Entire	900%	Philips Briliance 64	120	B	n

23	7	8	1.43	Middle shaft	F	B	42	63	158	L	Entire	170-380%	Philips Briliance 64	120	C	n
24	10	10	0.70	Neck	F	TCC	74	52	155	R	89 mm Proximal	22%	Philips Mx8000 IDT 16	120	B	y
25	11	11	1.56	Neck	F	B	63	160	182	L	Entire	140%	Siemens iCT 256	120	B	y
26	9	9	0.87	Neck	M	MM	79	65	165	R&L	145, 144 mm Proximal	178%	Philips Briliance 64	120	C	y
27	11	12	.1.67	Neck	F	B	65	87	150	R	Entire	140%	Philips Gimini TF Top 16	120	B	y
28	9	9	1.30	Neck	F	MM	69	65	160	L	84-60 mm Proximal	19%	Philips Briliance 64	120	B	y
29	10	10	1.45	Neck	F	B	70	62	162	R	About 30 cm		Philips Briliance 64	120	B	y
30	9	9	2.18	Neck	F	RCC	77	65	165	R	Entire		Siemens iCT 256	120	B	y
31	9	10	3.29	Proximal shaft	M	L	54	61	170	L	Entire		Philips Briliance 64	120	B	n
32	7	6	1.00	Distal shaft	F	B	39	70	170	L	Entire	10%	Philips Briliance 64	120	B	n
33	10	9	3.63	Proximal shaft	F	MM	61	51	155	L	Entire	huge	Phillips iCT256	120	B	y
34	11	10	2.85	Proximal shaft	F	AI	76	53	153	R	Entire	huge	Philips iCT256	120	idose(3)	y

35	10	10	1.40	Middle shaft	M	RCC	54	106	?	R	Entire	more 200%	Philips Briliance 64	120	B	y
36	10	10	1.30	Neck	F	L	50	56	152	R	110 mm	66%	Philips Briliance 64	120	B	y
37	11	10	1.61	Neck	F	B	60	60	158	R	107 mm	130%	Philips Briliance 64	120	B	y
38	9	9	5.12	Distal shaft	F	B	57	80	170	R	Entire	huge	Philips Briliance 64	120	B	y
39	10	10	3.14	Proximal shaft	F	B	69	75	?	R	Entire	huge	Philips iCT256	120	B	n
40	7	8	1.23	Proximal shaft	M	Colon	26	45	?	R	Entire	48%	Philips iCT256	120	B	n
41	9	9	3.04	Distal shaft	F	AI	59	80	165	L	Entire	100%	Philips iCT256	120	B	n
42	8	?	0.97	Middle shaft	M	L	53	140	?	L	Entire	10%	Philips Briliance 64	120	B	y
43	8	?	0.94	Neck	M	MM	64	65	?	R	Entire	300%	Philips Briliance 64	120	A	n
44	?	?	0.63	Neck	F	MM	64	78	153	R	Entire	10%	Philips iCT256	120	A	n
45	9	?	1.73	Middle shaft	M	MM	67	78	175	R	Entire	83%	Philips iCT256	120	B	y

* n - No pathological fracture within a period of 4 months only

** B – Breast, MM – Multiple myeloma, L – Lung, RCC – Renal cell cancer, P – Prostate, AI – Adenocarcinoma intrauterine, O – Other

Appendix B – Group 1 radiographs and CTFEAs.

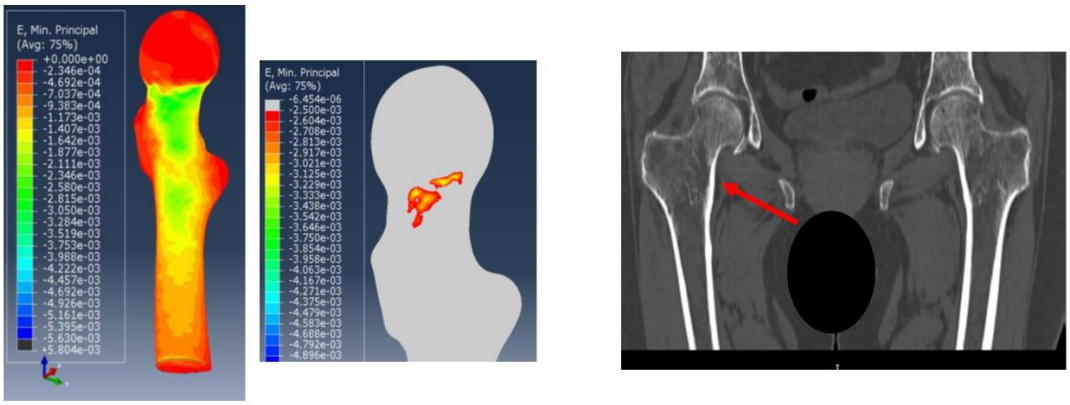

Figure B.1 –CTFEA and radiographs of a 59 y.o., 68kg female with multiple myeloma metastatic tumor at neck in the right femur with a Mirels' score of 9 and an estimation of a low risk of fracture (patient pathological fracture 1) but the CTFEA predicted a risk of fracture (max strain 4080 μstrain, typical strain fold change 1.48). The patient experienced a pathological fracture after the CT scan. Left) CTFEA model and maximum principal tensile strains at 2.5 body weights stance position. Colors represent the maximum compressive principal strains. Right) Radiograph prior to pathological fracture.

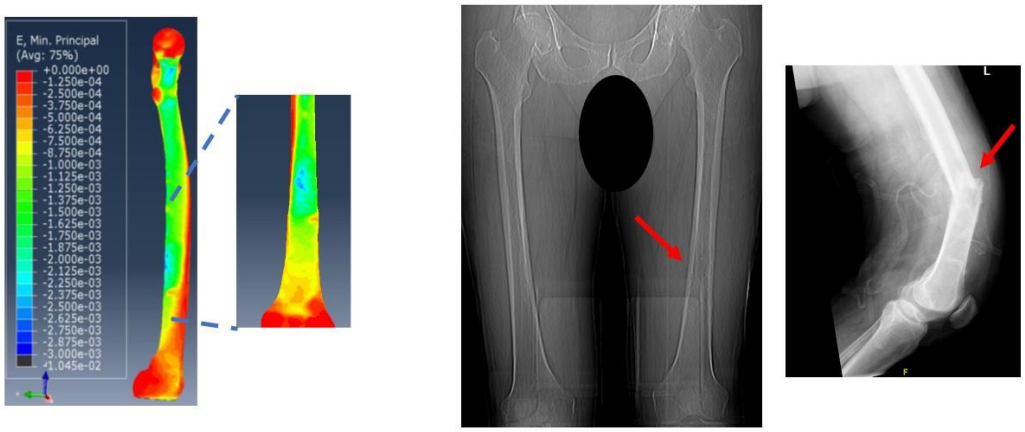

Figure B.2 –CTFEA and radiographs of a 75 y.o., 75kg male with multiple myeloma metastatic tumor at the left medial mid shaft with a Mirels' score of 7-8 and an estimation of a low risk of fracture (patient pathological fracture 2) but the CTFEA predicted a risk of fracture (max strain 2500 μstrain, typical strain fold change 2.27). The patient experienced a pathological fracture after the CT scan. Left) CTFEA model and maximum principal compressive strains at 2.5 body weights stance position. Right) Radiographs prior and following pathological fracture.

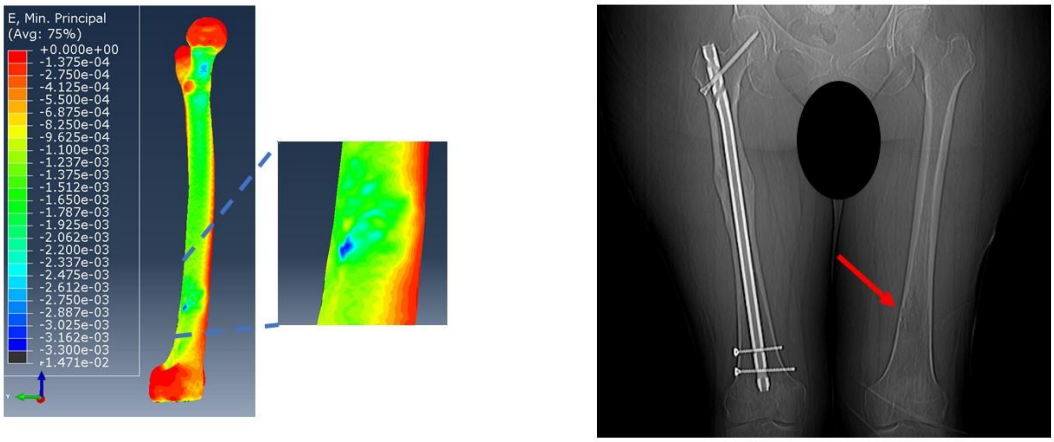

Figure B.3 –CTFEA and radiographs of a 68 y.o., 62kg female with multiple myeloma metastatic tumor at the left medial distal shaft with a Mirels' score of 7-8 and an estimation of a low risk of fracture (patient pathological fracture 3) but the CTFEA predicted a risk of fracture (max strain 2500 µstrain, typical strain fold change 2.27). The patient experienced a pathological fracture after the CT scan. Left) CTFEA model and maximum principal compressive strains at 2.5 body weights stance position. Right) Radiographs prior to fracture.

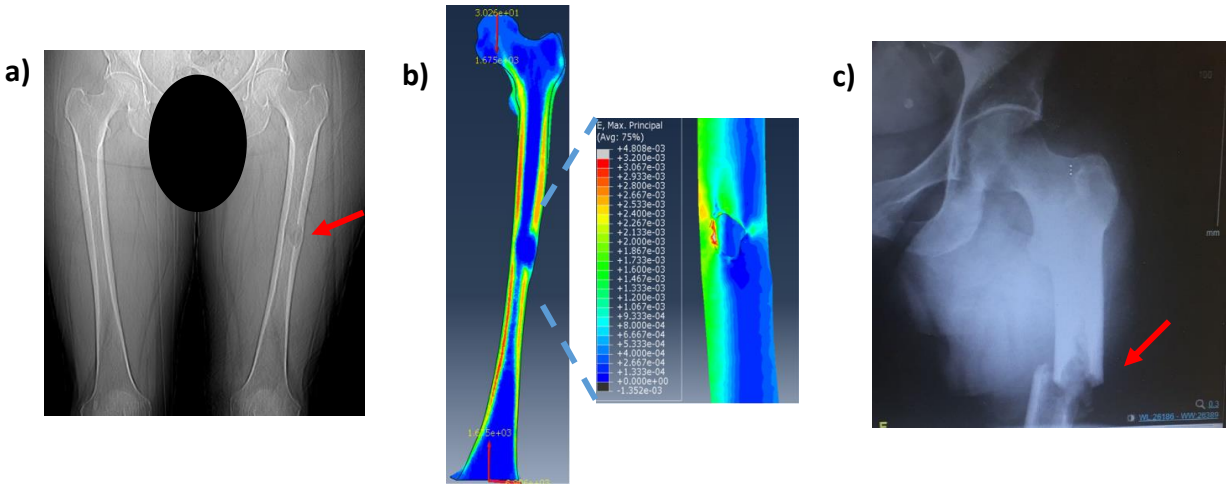

Figure B.4 (Same as Figure 4 in the manuscript) – Radiographs and CTFEA of a 54 y.o., 67kg female with uterine sarcoma (lytic) tumor in mid diaphysis in the left femur with a Mirels' score of 8 and an estimation of a low risk of fracture (patient pathological fracture 4) but the CTFEA predicted a high risk of fracture (max strain 3500 µstrain, typical strain fold change 1.89). The patient experienced a pathological fracture within 3 weeks after the CT scan. a) Radiograph prior to fracture, b) CTFEA model and maximum principal tensile strains at 2.5 body weights stance position. Colors represent the maximum tensile principal strains – hot colors are high strains. c) Radiograph after the pathological fracture.

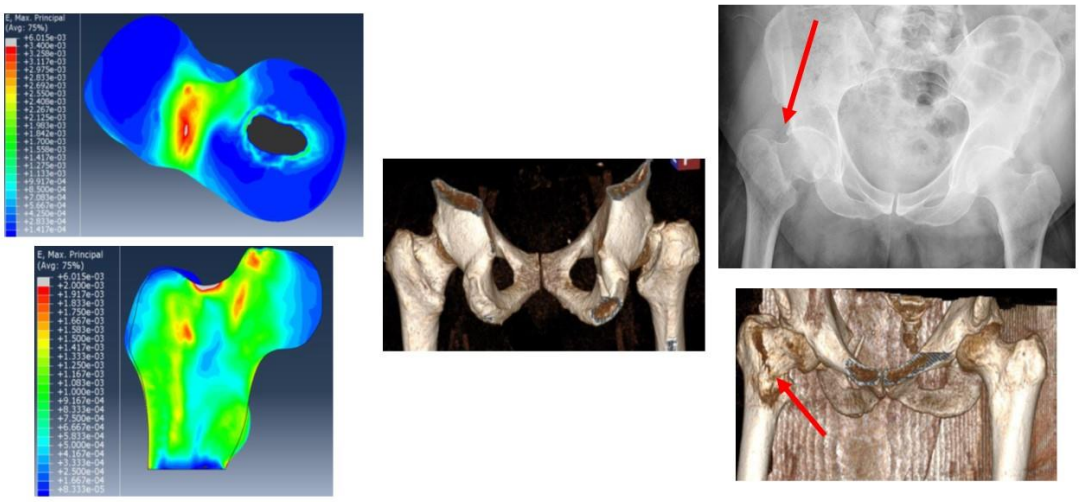

Figure B.5 –CTFEA, 3D reconstruction of CT scan and radiographs of a 62 y.o., 90kg male with lung metastatic tumor at the neck in the right femur with a Mirels' score of 8 and an estimation of a low risk of fracture (patient pathological fracture 5) but the CTFEA predicted a high risk of fracture (max strain 4700 μstrain, typical strain fold change 1.71). The patient experienced a pathological fracture after the CT scan. Left) CTFEA model and maximum principal tensile strains at 2.5 body weights stance position. Colors represent the maximum tensile principal strains – hot colors are high strains. Middle) 3D reconstruction of CT scan prior to fracture, Right) Radiograph and 3D reconstruction of CT scan after the pathological fracture.